Co-production of 1,3 propanediol and long-chain alkyl esters from crude glycerol

Rahul Mangayil [a, *], Elena Efimova [a], Jukka Konttinen [a], Ville Santala [a]

[a] Bio and Circular Economy Research Group, Faculty of Engineering and Natural Sciences, Hervanta Campus, Tampere University, Tampere, Finland

E-mail: Rahul Mangayil, rahul.mangayil@tuni.fi; Elena Efimova, elena.efimova@tuni.fi; Jukka Konttinen, jukka.konttinen@tuni.fi; Ville Santala, ville.santala@tuni.fi

[*] Corresponding author

Abstract

Crude glycerol is an excellent carbon source for bacterial production systems. Bacterial fermentation often generates by-products that can offer an additional carbon pool to improve the product profile for optimal valorization. In this study, the properties of two phylogenetically distinct bacteria, *Acinetobacter baylyi* ADP1 and *Clostridium butyricum*, were coupled in a one-pot batch process to co-produce 1,3 propanediol (PDO) and long-chain alkyl esters (wax esters, WEs) from crude glycerol. In the process, *A. baylyi* deoxidized the growth medium allowing glycerol fermentation and PDO production by *C. butyricum*. Reaeration of the co-cultivations enabled *A. baylyi* to metabolize the fermentation by-products, acetate and butyrate, and synthesize intracellular WEs. To improve PDO production and *A. baylyi* growth, carbon and macronutrients in the growth medium were screened and optimized using Plackett-Burman and Box-Behnken models. The validation experiment revealed a good correlation between the observed and predicted values. The salting-out method recovered 89.5% PDO from the fermentation broth and *in vacuo* extraction resulted in a PDO content of 5.3 g L^{-1}. Nuclear magnetic resonance revealed a WE content and yield of 34.4±1.4 mg L^{-1} and 34.2±3.2 mg WE g^{-1} dry cell weight, respectively. A molar yield of 0.65 mol PDO mol^{-1} and 0.62 µmol WE mol^{-1} crude glycerol was achieved with the synthetic consortium. This work emphasizes the strength of response surface methodology in improving production processes from the mutualistic association of divergent bacterial species in consortium. The co-production of PDO and WEs from crude glycerol is demonstrated for the first time in this study.

Keywords

Abbreviations

PDO, 1,3 propanediol; WEs, Wax esters; *A. baylyi* ADP1, *Acinetobacter baylyi* ADP1; *C. butyricum,* *Clostridium butyricum*; *C. kluyveri*, *Clostridium kluyveri*; *E. coli*, *Escherichia coli*; spp., species; NaCl, Sodium chloride; $(NH_4)_2SO_4$, Ammonium sulfate; $MgSO_4.7H_2O$, Magnesium sulfate heptahydrate; $CaCl_2.2H_2O$, Calcium chloride dihydrate; $ZnCl_2$, Zinc chloride; $MnCl_2.4H_2O$, Manganese chloride tetrahydrate; H_3BO_3, Boric acid; $CoCl_2.6H_2O$, Cobalt chloride hexahydrate; $CuCl_2.2H_2O$, Copper chloride dihydrate; $NiCl_2.6H_2O$, Nickel chloride hexahydrate; $FeSO_4.7H_2O$, Ferrous sulfate heptahydrate; $Na_2MoO_4.2H_2O$, Sodium molybdate dihydrate; H_2SO_4, Sulfuric acid; OD_{600nm}, Optical density measured at 600 nm; TE, Trace element; h, Hours; ANOVA, Analysis of variance; ^1H NMR, Proton nuclear magnetic resonance; HPLC, High performance liquid chromatography; NAD^+ and NADH, Oxidized and reduced form of nicotinamide adenine dinucleotide; DCW, Dry cell weight.

Introduction

Biodiesel derived from the transesterification of triglycerides represents one of the sustainable alternatives to petroleum diesel. However, it is important to address the proportionally equivalent amounts of crude glycerol generated from the oleochemical industries (1 kg glycerol from 10 kg biodiesel). This glut of crude glycerol, caused by the excess of supply over demand, has lowered the global glycerol price to $0.33 kg^{-1} ($0.03 mol^{-1}), making it competitive with that of sugars [1–3]. Crude glycerol is an excellent carbon source from which to produce a variety of high-value compounds such as hydrogen, 1,3 propanediol (PDO), ethanol, glutamate and polyhydroxyalkanoates [4–7]. Of these, research has mainly focused on PDO production.

The global demand for PDO as a precursor chemical for synthesis of polymers such as polyethers, polyurethanes and polyesters is rapidly growing [8]. PDO currently sells for $35 kg^{-1} ($2.7 mol^{-1}) [9]. Based on a recent survey, the market value of PDO is projected to $621.2 million by 2021 [10]. PDO

3

can be produced through chemical synthesis from petroleum-derived compounds such as acrolein and ethylene oxide [11,12], and via bioconversion routes. Bioconversion of crude glycerol to PDO has been reported via anaerobic and micro-aerobic fermentations using pure and recombinant bacterial strains, and mixed microbial communities. Among the pure strains, *Clostridium butyricum* is the most efficient native producer, reported to generate PDO titers of ~90 g L^{-1} with molar yields of 0.5 - 0.6 mol mol^{-1} substrate [13,14]. In addition to PDO, glycerol fermentation by *Clostridium* spp. generates other products such as acetate, butyrate, butanol, ethanol and lactate. Efforts have been made to enhance the carbon flow towards the target product, by using classical strain improvement [15] and process optimizations [16]. However, these by-products can serve as an additional carbon pool to augment glycerol valorization. In one study, co-generation was demonstrated of PDO and caproate from glycerol and fermentation by-products, respectively, via the synergistic association of *C. butyricum*, *Escherichia coli*, and *C. kluyver*i present in an anaerobic digesting sludge [17]. Another example described an unconventional strategy for the combined production of PDO and polyhydroxyalkanoates from crude glycerol using anaerobic sludge [3].

The present study focused on linking the metabolic activities of two divergent microbial species for the coupled generation of PDO and long-chain alkyl esters (wax esters, WEs) from crude glycerol. The WEs, oxoesters of long-chain fatty acids esterified with long-chain alcohols, are exploited in a multitude of applications such as in, for example cosmetics, lubricants, and food industries. A major share of the global WE supply relies on plant sources, such as jojoba oil, which is priced at $55 kg^{-1} ($27 mol^{-1}) [18]. The market value of jojoba oil is forecasted to reach $254 million by 2024 [19]. Certain bacterial genera such as *Acinetobacter* and *Rhodococcus* can natively synthesize WEs as an energy reserve compound. In contrast to plants, microbial WE production systems benefit from using wide range of substrates and rational genetic engineering strategies for efficient carbon channeling [20–22]. In bacteria, WE synthesis commences through the natural lipid metabolism pathway. Acetyl CoA derived from the carbon source

undergoes a series of reduction steps generating fatty alcohol, which is esterified with fatty acyl-CoA to form WEs. Accumulation of WE in *Acinetobacter* spp. occurs under carbon-excess conditions and is associated with cell growth [23]. Under carbon-limited conditions, the accumulated WEs are degraded for biomass formation. In addition to model substrates, WE synthesis from fermentation metabolites using rationally designed co-cultures have been reported. Metabolisms of *E. coli* and *A. baylyi* mutant were linked to redirect the carbon in acetate (produced by *E. coli*) towards biomass and WE accumulation in *A. baylyi* cells [24]. A one-pot batch process was recently demonstrated for the co-production of H_2 and WEs by pairing the metabolic properties of *C. butyricum* and an *A. baylyi* ADP1 mutant [25].

In the present study, the innate fermentation capability of *C. butyricum* and the aerobic synthesis of *A. baylyi* ADP1 were exploited to cogenerate PDO and WEs from crude glycerol. Plackett-Burman model and Box-Behnken design were employed to improve PDO and WE production. The experimental design included carbon source and macronutrients in the growth medium, and PDO and *A. baylyi* ADP1 growth as model variables and responses, respectively. The model was validated in the predicted optimal medium composition and the products were recovered from the fermentation broth for analysis. This is the first evidence of PDO and WE coproduction from crude glycerol in a one-pot batch cultivation.

Materials and Methods

Chemicals and glycerol source

NaCl, K_2HPO_4, $(NH_4)_2SO_4$, $MgSO_4.7H_2O$, $CaCl_2.2H_2O$, and trace element chemicals $ZnCl_2$, $MnCl_2.4H_2O$, H_3BO_3, $CoCl_2.6H_2O$, $CuCl_2.2H_2O$ and $NiCl_2.6H_2O$ were from Merck (Germany). Tryptone and yeast extract were from Lab M Limited (UK). $FeSO_4.7H_2O$ was from VWR International (USA) and $Na_2MoO_4.2H_2O$ was from J T Baker (USA).

Crude glycerol was generously provided by Perstrop AB (Sweden). This crude glycerol, obtained from the transesterification of rapeseed oil, had a slightly acidic pH (6.0) and contained 80% glycerol, 3% non-glycerol organic matter and 3% ash.

Bacterial strains and cultivation conditions

Wild type *A. baylyi* ADP1 (DSM 24193, Germany) and *C. butyricum*, isolated from a hydrogen-producing bioreactor [26], were used in this study. The pre-inocula of *A. baylyi* and *C. butyricum* were prepared by inoculating the cells in aerobic low salt lysogenic broth (10 g L^{-1} tryptone; 5 g L^{-1} yeast extract; 5 g L^{-1} NaCl) and anoxic Reinforced Clostridial Medium (Merck, Germany), respectively. The bacterial strains were grown overnight at 30^oC and 300 rpm.

The batch process and *in unison* microbial inoculations were conducted as described previously [25]. Briefly, 400µl of pre-cultivated *A. baylyi* ADP1 cells (OD_{600nm} of 2.5) were inoculated into 50 ml of minimal medium (JM medium; 1.5 g L^{-1} K_2HPO_4, 2.0 g L^{-1} $(NH_4)_2SO_4$, 0.2 g L^{-1} $MgSO_4.7H_2O$, 0.015 g L^{-1} $CaCl_2.2H_2O$, 0.005 g L^{-1} $FeSO_4.7H_2O$, and 0.3 g L^{-1} yeast extract). The medium was supplemented with 2 ml L^{-1} of TE solution containing 1 ml L^{-1} of 25% HCl and the following compounds: 0.07 g L^{-1} $ZnCl_2$, 0.1 g L^{-1} $MnCl_2.4H_2O$, 0.06 g L^{-1} H_3BO_3, 0.2 g L^{-1} $CoCl_2.6H_2O$, 0.02 g L^{-1} $CuCl_2.2H_2O$, 0.02 g L^{-1} $NiCl_2.6H_2O$, and 0.04 g L^{-1} $Na_2MoO_4.2H_2O$. To initiate *A. baylyi* and *C. butyricum* growth, the medium was supplemented with 10 mM acetate and crude glycerol, respectively. The inoculated bottles were closed with sterile rubber stoppers and tightened with aluminum crimps. Pre-grown *C. butyricum* cells (400µl of OD_{600nm} 2.7) were aseptically added to the cultivation vessel containing *A. baylyi* cells.

Preliminary experiments to investigate the substrate utilization and the requirement for acetate supplementation in *A. baylyi – C. butyricum* co-cultures were conducted in a crude glycerol (5 g L^{-1}) amended JM medium with and without acetate (10 mM) in the cultivation set-up as described above. The co-cultures were grown at 30^oC and 300 rpm for 24 h, establishing the anaerobic phase, after which the cultures were transferred to sterile Erlenmeyer flasks and grown for another 12 h (aerobic phase). A

cultivation devoid of bacterial cells was included as experimental control. The medium pH was not adjusted during the experiment. Samples for analysis (pH, substrate and metabolites concentrations and cell growth) were collected at specified intervals.

Experimental design

The effects of macronutrients in the growth medium and carbon substrate were evaluated for the improvements in PDO and WE production in batch. In this work, the carbon in the fermentation by-products, acetate and butyrate, was directed towards *A. baylyi* biomass and WE production. Thus, for the optimization studies, both PDO production and *A. baylyi* ADP1 growth were included as model responses. The macronutrients in JM medium (above) and crude glycerol were chosen as variables. The statistical models were designed in Minitab 17.0 (USA). R^2 and adjusted R^2 values were calculated using equations 1 and 2.

$$R^2 = 1 - \left[\frac{SS_{residual}}{SS_{total} - SS_{curvature}} \right] \qquad \text{(eq. 1)}$$

where $SS_{residual}$ is the adjusted sum of square (Adj SS) of the model error, SS_{total} is the total Adj SS and $SS_{curvature}$ is the Adj SS of the model curvature.

$$Adjusted\ R^2 = 1 - \left[\frac{SS_{residual}}{df_{residual}} \right] \Big/ \left[\frac{SS_{total} - SS_{curvature}}{df_{total} - df_{curvature}} \right] \qquad \text{(eq. 2)}$$

where df is the degree of freedom and $\frac{SS_{residual}}{df_{residual}}$ represents the adjusted mean square of the model error.

The experiments were carried out in 50 ml JM medium containing altered medium compositions as suggested by the implemented models. The co-cultivation set-up for all the optimization tests was as described above.

Plackett-Burman

Plackett-Burman was employed to screen and identify the variables that had significant effects on the model responses [27]. Plackett-Burman is based on the first order polynomial model,

$$Y = \beta_0 + \Sigma \beta_i X_i \qquad\qquad (eq. 3)$$

where Y is the response, β_0 is the model intercept, β_i is the linear coefficient and X_i is the level of an independent variable.

For the construction of the model, variable concentrations at high (+1) and low (-1) levels were kept at twice and half their corresponding values in the original medium composition (above). The generated design (**Table 1**) contained 14 randomized experimental runs, with three runs at the center points (0; original JM medium composition). The uncoded +1, 0 and -1 values were : 3, 1.5 and 0.75 g L^{-1} K_2HPO_4; 4, 2 and 1 g L^{-1} $(NH_4)_2SO_4$; 0.4, 0.2 and 0.1 g L^{-1} $MgSO_4.7H_2O$; 0.03, 0.15 and 0.0075 g L^{-1} $CaCl_2.2H_2O$; 0.01, 0.005 and 0.0025 g L^{-1} $FeSO_4.7H_2O$; 10, 5 and 2.5 g L^{-1} crude glycerol.

The ANOVA selected model variables with statistically significant (p-value ≤ 0.04) effect. Since PDO production and *A. baylyi* growth is influenced by the metabolic pairing between the bacterial species, variables with significant effects on both responses were analyzed. Multiple response optimizer tool was chosen to predict solutions facilitating maximal PDO production and *A. baylyi* ADP1 growth.

Box-Behnken

$FeSO_4.7H_2O$, K_2HPO_4 and $(NH_4)_2SO_4$, selected from the Plackett-Burman experiments were optimized using a three-variable Box-Behnken design with PDO and *A.baylyi* ADP1 growth as responses [28]. **Table 2** presents the randomized design. The uncoded +1, 0 and -1 values were: 0.1, 0.055 and 0.01 g L^{-1} $FeSO_4.7H_2O$; 6, 4.5 and 3 g L^{-1} K_2HPO_4; 1, 0.75 and 0.5 g L^{-1} $(NH_4)_2SO_4$.

The ANOVA analyzed the statistical significance of the model terms on each response. The observed data points were fitted through response surface regression using the second order polynomial equation,

$$Y = \beta_0 + \sum \beta_i X_i + \sum \beta_{ii} X_i^2 + \sum \beta_{ij} X_i X_j \qquad\text{(eq. 4)}$$

where Y is the predicted response, X_i and X_j are independent variables, β_0 a constant, β_i linear coefficients, β_{ii} quadratic coefficients, and β_{ij} the cross-product coefficient.

Validation experiment

The validation experiments were conducted in optimized JM medium (4.0 g L^{-1} K$_2$HPO$_4$; 0.54 g L^{-1} (NH$_4$)$_2$SO$_4$; 0.4 g L^{-1} MgSO$_4$.7H$_2$O; 0.0075 g L^{-1} CaCl$_2$.2H$_2$O; 0.01 g L^{-1} FeSO$_4$.7H$_2$O; 10 g L^{-1} crude glycerol; 0.3 g L^{-1} yeast extract; 2 ml L^{-1} TE solution and 10 mM acetate). The co-cultivation was conducted as described above.

For the PDO and WE analysis, *A. baylyi* and *C. butyricum* cocultures were grown in 500 ml serum bottles containing a working volume of 300 ml of the optimized JM medium. Until the anaerobic phase, the cultivation set-up was as previously described. After analyzing the headspace gaseous composition, the bottles were opened, ensuring resupply of air and utilization of the fermentation by-products by *A. baylyi* cells, and the cultures were grown at 30$^\mathbf{o}$C and 300 rpm.

Analytical methods

Bacterial growth was measured as OD$_{600nm}$ using an Ultrospec 500 pro spectrophotometer (Amersham Biosciences, UK). The medium pH was analyzed using 330i pH meter (WTW, USA). Lipid extraction from the freeze-dried biomass and quantitative ^{1}H NMR analysis of the WEs were performed as previously described [25]. To calculate the WE content (mg L^{-1}), an average WE molar mass of 506 g mol^{-1} (corresponding to WE molecule with 34 C atoms and one double bond) was used [29]. Glycerol, PDO, acetate and butyrate in the cultivation medium were analyzed using an LC-20AD prominence liquid chromatograph (Shimadzu, Japan), equipped with a Rezex^{TM} RHM-Monosaccharide H$^+$ column (300×8 mm; Phenomenex, USA), an RID-10A Shimadzu refractive index detector and a mobile phase of

0.01N H_2SO_4 as described in [30]. The molar yields (mol PDO mol^{-1} crude glycerol) were calculated by dividing the PDO concentration (mM) by the utilized crude glycerol content (mM).

PDO in the fermentation broth was extracted and the recovery yield was calculated as described in [31].

Results and Discussion

Suitability of A. baylyi ADP1 in assisting C. butyricum fermentation

We have previously shown *A. baylyi* ADP1 to deoxygenize and remove *C. butyricum* growth inhibitors, facilitating H_2 production from rice straw hydrolysate [32]. In a recent study, 'metabolic pairing' was established between *C. butyricum* and *A. baylyi* mutant for the co-generation of H_2 and WEs [25]. Here, the suitability of *A. baylyi* to assist *C. butyricum* in crude glycerol (5 g L^{-1}) fermentation was studied in an oxic JM medium with and without acetate (10 mM). After a 24 h cultivation period, bacterial growth was not observed in the JM medium without acetate supplementation. *A. baylyi* ADP1 cells cannot natively metabolize glycerol [33]. The absence of a suitable carbon source (acetate) in the oxic cultivation medium restricted *A. baylyi* cells in biomass formation and medium deoxygenation, thereby limiting *C. butyricum* fermentation. In the case of acetate-added medium, *C. butyricum* in the co-culture produced PDO (20.1±0.9 mM), acetate (2.6±0.0 mM) and butyrate (3.8±0.1 mM), utilizing 52% (2.6 g L^{-1}) of crude glycerol. The supply of air after the anaerobic phase established the aerobic phase (12 h), permitting the *A. baylyi* cells to utilize acetate and butyrate. These results demonstrates metabolic pairing in acetate-added JM medium. Rationally designed microbial consortia allow to build systems with metabolic capacities surpassing those of single-cell cultures. For instance, a three-species 'cross-feeding' consortium was designed comprising of *E. coli*, *Bacillus subtilis* and *Shewanella oneidensis* to generate electricity from glucose [34]. In that community, *E. coli* converted glucose to lactate, which was oxidized by *S. oneidensis*. *S. oneidensis* in turn produced acetate feed for *B. subtilis* and *E. coli* cells. *B. subtilis* produced riboflavin, an electron shuttle required for electricity generation by *S.*

10

oneidensis. Another study reported a starch-sucrose based L-lysine production by a sucrose-negative α-amylase-secreting *E. coli* strain and a fructose-secreting L-lysine-producing *Corynebacterium glutamicum* strain [35]. These studies shed light on how non-native production routes can be achieved through mutualistic association of bacterial species in synthetic consortia.

Screening for medium components that have significant effects on PDO production and A. baylyi ADP1 growth

The effects of the JM medium components, K_2HPO_4, $(NH_4)_2SO_4$, $MgSO_4.7H_2O$, $CaCl_2.2H_2O$, $FeSO_4.7H_2O$, and crude glycerol concentrations on PDO production and *A. baylyi* ADP1 growth were studied using Plackett-Burman design. The incomplete utilization of the substrate by *C. butyricum* cells after a 24 h cultivation period (above) suggested to extend the anaerobic phase to 48 h. Table 1 presents the results from the Plackett-Burman runs. After 48 h, *C. butyricum* completely metabolized 2.5 and 5 g L^{-1} crude glycerol. At 10 g L^{-1}, the substrate utilization ranged from 46±0.1% in Run 4 to 68±0.3% in Run 14. This can be attributed to a non-optimal nutrient content in the growth medium and operational conditions, such as pH, cultivation temperature and fermentation period, all of which have been reported to influence *C. butyricum* fermentation [36–39]. In Run 14, *C. butyricum* metabolized 68% of the substrate producing 52.3±1.8 mM PDO, 7.3±0.1 mM acetate and 11±0.5 mM butyrate. Apart from Runs 2, 7 and 10, *A. baylyi* utilized acetate and butyrate for growth (OD_{600nm} 0.3±0.0 to 1.2±0.1), indicating that the growth restrictions can be attributed to the low medium pH (pH 5.1).

The ANOVA data from PDO production and *A. baylyi* ADP1 growth models are shown in **Table 3** and the linear regression equations are presented in equations 5 and 6, respectively.

$$PDO = 13.74 + 0.59\,K_2HPO_4 - 0.643\,(NH_4)_2SO_4 - 2.74\,MgSO_4.7H_2O - 50.1\,CaCl_2.2H_2O +$$
$$183\,FeSO_4.7H_2O + 3.5186\,Crude\,glycerol + 11.029\,Ct\,Pt \qquad\qquad (eq.\ 5)$$

$$A. baylyi\ ADP1\ growth\ = 0.154 + 0.3156\ K_2HPO_4 - 0.1944\ (NH_4)_2SO_4 + 0.861\ MgSO_4.7H_2O -$$

$$8.44\ CaCl_2.2H_2O - 3.56\ FeSO_4.7H_2O + 0.01667\ Crude\ glycerol + 0.6789\ Ct\ Pt \qquad \text{(eq. 6)}$$

The model F-value and the 'lack-of-fit' determines the association of the variable with the response and the fitness of the model, respectively. The model factors with p-value ≤ 0.04 indicates that there is only a 4% chance that the significance is due to error. The degree of significance is evaluated based on its effect, either positive or negative, towards the response.

The PDO production as the response variable resulted in a model with an F-value and a p-value of 360.51 and <0.01, respectively. The fitted model showed minimal variation (S-value 0.9 mM, standard deviation in uncoded response values) between the experimental and predicted values (Table 1). The correlation coefficient of 0.998 for the regression equation implies that 99.8% variability in PDO production could be explained with the model. The R^2 value was in reasonable agreement with the adjusted R^2 (99.5%), indicating the model fitness. A p-value of 0.047 indicates a slight chance (4.7 %) that the model 'lack-of-fit' is significant. As indicated by the model coefficients, K_2HPO_4, and crude glycerol had a significant positive effect on PDO production, whereas $(NH_4)_2SO_4$ showed a negative effect on the response. The observed positive effects of K_2HPO_4 relates to the importance of phosphate and potassium in cellular biosynthesis. Potassium ions constitute the main inorganic cellular cation and as a cofactor in enzyme function. Phosphate is an integral component for nucleic acid, nucleotide and phospholipid biosynthesis. This suggests that higher K_2HPO_4 concentrations can improve phosphate and potassium availability in the medium and thereby improve metabolic activities.

For *A. baylyi* ADP1 growth, a regression model with an F-value of 38.41 and a p-value of <0.01, an insignificant lack-of-fit (p-value = 0.23) and an S-value of 0.1 OD_{600nm} was obtained. The R^2 value of the model was in reasonable agreement with the adjusted R^2 of 95.2%. Crude glycerol displayed a negligible effect (F-value, 3.16; p-value, 0.13) while $(NH_4)_2SO_4$ and $CaCl_2.2H_2O$ showed significant negative effects, and K_2HPO_4 and $MgSO_4.7H_2O$ had a positive influence on *A. baylyi* ADP1 growth.

12

Crude glycerol was expected to affect *A. baylyi* growth as the carbon sources, acetate and butyrate, are derived from the substrate. Since the fermentation by-products were not included as variables in the experimental design, the model did not analyze their contribution to the response.

Another factor is the initial acetate content. Acetate (10 mM) was supplemented to promote *A. baylyi* growth and medium deoxygenation. In addition to biomass formation, acetate also contributes slightly towards WE accumulation [25]. This contribution was taken into account during the model analysis. The observed response (*A. baylyi* ADP1 growth, OD_{600nm}) reported in Table 1 is the value wherein the cell densities obtained after the 48 h anaerobic phase (containing *A. baylyi* cells grown with initial acetate and *C. butyricum* cells) were subtracted from the final OD_{600nm} data.

The presence of curvature (p-value ≤ 0.04) in the PDO and *A. baylyi* ADP1-fitted models (Table 3) suggests a curvilinear relationship between the tested variables, indicating the need for further optimizations. The predicted solution with the highest desirability score (Solution 1 in Table A1), was chosen as basis to construct the Box-Behnken design.

Box-Behnken optimization

Based on the ANOVA results from the Plackett-Burman models, K_2HPO_4 and $(NH_4)_2SO_4$ were selected for the next optimization tests. In the Plackett-Burman PDO production model, a p-value (0.05) slightly higher than the threshold was observed for $FeSO_4.7H_2O$ (Table 3). However, as $FeSO_4$ imparted the second highest positive effect after crude glycerol it was decided to include $FeSO_4$ in the Box-Behnken design. Evaluating the significance and effect of $MgSO_4.7H_2O$ and $CaCl_2.2H_2O$ on both responses, the concentrations were maintained at 0.4 g L^{-1} and 0.0075 g L^{-1}, respectively. Due to the incomplete substrate utilization observed from Plackett-Burman experiments, crude glycerol was omitted from the design and was retained at 10 g L^{-1}.

Table 2 presents the results from Box-Behnken experimental runs. Compared to the Plackett-Burman data, the experimental runs resulted in higher glycerol utilization ($78.3\pm0.9\%$ – $87.9\pm2.5\%$), PDO production

(53.0±0.6 mM – 58.5±3.1 mM). The medium pH after anaerobic phase averaged around 6.5 (pH 6.3 – 6.7). This favorable growth pH allowed *A. baylyi* cells to completely utilize the acetate and butyrate and grow to an OD_{600nm} ranging from 0.8±0.1 – 1.9±0.0.

The PDO production model showed a low F-value (0.92) and p-value (0.53), indicating an insignificant relation between the selected variables and the response (**Table 4**). The prediction error sum of squares (PRESS) measures the statistical fitness between the predicted and observed response values. The lower the PRESS score, the better the model fits to the experimental data. For the PDO production model a PRESS score of 321.0 and an S-value of 2.6 mM were obtained. Nevertheless, the insignificant lack-of-fit (p-value = 0.5), suggests that the model shows a reasonable fit with the obtained results. In the Plackett-Burman model, crude glycerol had the greatest relation with PDO production (Table 3). Due to the incomplete utilization and the expected substrate-related inhibitory effects on bacterial growth [40], crude glycerol was excluded from the design. This is justified by obtaining an insignificant model with limited variable interactions to the response.

In the case of *A. baylyi* ADP1 growth, a significant model (p-value <0.01) with a 'lack-of-fit F-value', PRESS score and an S-value of 0.86, 1.6, 0.2 OD_{600nm}, respectively was obtained (Table 4). The correlation coefficient of the polynomial equation suggested that the model could explain only 70% of the variability in *A. baylyi* growth. This could be due to the omission of other variables from the design. Significant linear and quadratic interactions between K_2HPO_4 and $(NH_4)_2SO_4$ on the response were observed from the ANOVA. The regression equation for *A. baylyi* ADP1 growth is presented in equation 7.

$A. baylyi$ ADP1 $growth = -2.69 + 9.18\ FeSO_4.7H_2O + 0.960\ K_2HPO_4 + 6.61\ (NH_4)_2SO_4 -$
$14.6\ FeSO_4.7H_2O * FeSO_4.7H_2O - 0.0548\ K_2HPO_4 * K_2HPO_4 - 2.63\ (NH_4)_2SO_4 * (NH_4)_2SO_4 -$
$1.43\ FeSO_4.7H_2O * K_2HPO_4 - 0.67\ FeSO_4.7H_2O * (NH_4)_2SO_4 - 0.677\ K_2HPO_4 *$
$(NH_4)_2SO_4$ (eq. 7)

In addition to the ANOVA statistics, the residual plots of the fitted model scrutinizes the distribution of experimental data and identifies for skewed or outlined data. The normal probability plot indicates that the residuals, i.e. the difference between the experimental and predicted values, are distributed linearly (**Figure 1**a). The residual versus predicted plot in Figure 1b shows a random distribution around the centerline, confirming absence of skewed or outlined residuals and goodness-of-fit of the model. For *A. baylyi* ADP1 response surface model, ridge-type contour plots were obtained (**Figure 2**a – c). The spaces between the contours indicate the degree of the effect on the response from the interaction between two variables [41]. The closer the contour lines, the steeper is the incline and *vice versa*. The contour curves in Figures 2a and 2b exhibited rising ridge patterns demonstrating the independent positive effect of $FeSO_4.7H_2O$ on *A. baylyi* growth and indicating maximal response with lower levels of K_2HPO_4 and $(NH_4)_2SO_4$. Nevertheless, the interactions between K_2HPO_4 and $(NH_4)_2SO_4$ indicated a slightly stationary ridge arrangement directing the peak maxima with low K_2HPO_4 and high $(NH_4)_2SO_4$ concentrations (Figure 2c).

Considering the focus of this study, i.e. to optimize the growth medium for enhanced PDO and WE production via synthetic coculture in a one-pot batch process, the direct retrieval of variable predictions from the regression equation is trivial. Therefore, the multiple response optimizer function including both the responses was employed. The predicted solution with the highest desirability score (Solution 1 in Table A2) was chosen for the validation experiment.

Model validation

The validation experiments were conducted in 50 ml of the optimized JM medium (4.0 g L^{-1} K_2HPO_4, 0.54 g L^{-1} $(NH_4)_2SO_4$, 0.4 g L^{-1} $MgSO_4.7H_2O$, 0.0075 g L^{-1} $CaCl_2.2H_2O$, 0.01 g L^{-1} $FeSO_4.7H_2O$, 10 g L^{-1} crude glycerol, 0.3 g L^{-1} yeast extract, 2 ml L^{-1} TE solution and 10 mM acetate). During the cultivation period, *C. butyricum* metabolized 95.0±2.0% of the crude glycerol producing 10.0±1.0 mM acetate, 12.2±1.0 mM butyrate and 66.1±2.3 mM PDO. The subsequent aerobic phase enabled *A. baylyi* ADP1

cells to utilize the fermentation by-products (9.1±1.1 mM acetate and 12.2±1.0 mM butyrate) and to grow to an optical density of OD_{600nm} 1.5±0.0. Inferring from the Box-Behnken data in Table 2, fermentation in the optimized JM medium led to improved PDO production (from 58.5±3.1 mM in Run 6 to 66.1±2.3 mM). The observed PDO concentration (66.1±2.3 mM) and *A. baylyi* ADP1 growth (OD_{600nm} 1.5±0.0) showed only 11% and 6% variations from the predicted values of 59.7 mM and OD_{600nm} 1.6, respectively (Table A2).

PDO and WE analysis from one-pot batch cultivation

To recover PDO and WEs, the cocultures were grown in 300 ml of the optimized JM medium at 30°C and 300 rpm. After 48 h, *C. butyricum* had consumed 110±5.0 mM crude glycerol producing 12.0±0.1 mM acetate, 17.0±0.0 mM butyrate and 72.0±0.2 mM PDO. *A. baylyi* cells completely metabolized the acetate and butyrate for biomass and WE synthesis (**Table 5**).

A salting-out method to extract PDO from the fermentation broth formed two layers (top layer, PDO in solvent; bottom layer, salts in water) separated with an interphase (proteins/cells). The HPLC analysis calculated 64.5 mM and 6.3 mM PDO in the top and bottom layers, respectively. The PDO recovery yield from the top phase was 89.5% and an *in vacuo* extraction resulted in a PDO content of 5.3 g L^{-1}. However, this is low when compared to previously reported values. For example, for cultivated *C. butyricum* VPI 1718 in fed-batch conditions, enhancements were observed in PDO production via process scale-up and reactor optimization (25 g L^{-1} in 1 L bioreactor to 32 g L^{-1} in 3 L bioreactor) [6]. In contrast, others have reported a drop in PDO content (76 g L^{-1} to 62 g L^{-1}) during a fed-batch bioreactor scale-up from 1 L to 200 L [13]. Furthermore, the cultivation temperature can affect PDO production. *A. baylyi* ADP1 grows at temperatures ranging from 30°C - 37°C, and optimally at 30°C [22]. For *C. butyricum*, growth is observed between 30°C - 40°C with the maximal PDO production at 33°C [14]. In an earlier report, the highest PDO concentrations of 10.1 g L^{-1} at 35°C were obtained using *C. butyricum* DSM 5431 grown in batch and a decrease in the PDO content was observed at lower temperatures (5.7 g

L^{-1} at 30°C) [39]. Differences in cultivation temperature, bioreactor geometries and process optimizations can be regarded as justifications for the PDO concentrations obtained with the production system used in this study.

In a two-stage system, in which the bacterial strains are grown separately, the physiological parameters influencing the cellular bioenergetics can be optimized to enhance single end-product formation. In contrast, a one-pot approach often limits such optimizations especially when microbes with distinct metabolisms are involved. Nevertheless, such processes offer other benefits. For instance, co-culturing *A. baylyi* and *C. butyricum* in a one-pot set-up eliminates the need for reducing agents for medium deoxygenation. Furthermore, such system aids in medium detoxification. Sustainable bioprocess substrates such as lignocellulosic biomass often include inhibitory compounds that can affect optimal cell growth. Medium detoxification can be achieved by designing a synthetic consortium consisting of bacteria capable to utilize such inhibitory compounds. For instance, an earlier publication demonstrated the capacity of *A. baylyi* cells to detoxify the inhibitors present in a rice straw hydrolysate, thereby assisting *C. butyricum* fermentation [32]. This benefit is restricted in the 2-stage process. Furthermore, one-pot system would be more productive as there would be medium deoxygenation, detoxification and product generation in same cultivation vessel.

In *C. butyricum*, glycerol is metabolized via oxidative and reductive routes [42]. The oxidative pathway (leading to biomass, ATP and pyruvate) generates reducing equivalents (NADH) that requires reoxidation in order to main the cellular redox balance. This is maintained through the reductive route in which NADH is oxidized to NAD$^+$ via PDO production pathway, preserving the synergy between the glycerol metabolism pathways. However, the pyruvate generated from the oxidative branch results in the formation of acetate and butyrate (competing NADH oxidizing pathway). Thus, a trade-off in the carbon pool between PDO production and WE synthesis (from the competing metabolic routes) is expected [43]. In this regard, the PDO content (5.3 g L^{-1}) obtained from this study is comparable to that reported

17

for glycerol-based co-production systems. For instance, a PDO content of 4.4 g L^{-1} from crude glycerol was reported during PDO-polyhydroxyalkanoate co-production using anaerobic sludge [4]. In a study to co-generate PDO and caproate from glycerol using anaerobic sludge, a PDO content ranging from 109 mM C (2.9 g L^{-1}) to 266 mM C (6.7 g L^{-1}) was reported [17].

Quantitative analysis of the long-chain alkyl esters produced by *A. baylyi* ADP1 cells revealed a WE content and yield of 34.4±1.4 mg L^{-1} and 34.2±3.2 mg WE g^{-1} DCW, respectively. In our previous study, a WE content and yield of 28 mg L^{-1} and 30 mg WE g^{-1} DCW was obtained using *C. butyricum* and *A. baylyi* mutant co-cultivated in an unoptimized JM medium [25]. The rational model design presented in this work aided to achieve higher acetate (12 mM) and butyrate (17 mM) concentrations. For instance, the acetate (5.1 mM) and butyrate (8.8 mM) obtained from the Plackett-Burman experiments (Runs 11-13, Table 1) were similar to those observed in our previous work. By screening and optimizing the medium composition, WE content and yield was improved by 23% and 14%, respectively.

A. baylyi does not natively metabolize glycerol. Nevertheless, a WE yield of 3.4 mg WE g^{-1} crude glycerol was obtained due to the one-pot nature of the overall process. This yield is competitive with that reported from other production systems in the literature. For instance, a yield of 0.75 mg WE g^{-1} glucose was obtained from *Saccharomyces cerevisiae* engineered to synthesize very long-chain alkyl esters [44]. In another example, WEs synthesized using an engineered *E. coli* strain from glucose and exogenous propionate, n-octanol and oleic acid supplementation yielded 2.5 mg WE g^{-1} glucose [45]. A comparable WE yield obtained from the present study via rational optimization highlights the bioprocess efficiency of the one-pot system with respect to other production processes.

Conclusions

This study establishes a proof-of-concept for the coupled production of PDO and WEs from crude glycerol using an *A. baylyi* ADP1 – *C. butyricum* co-culture in a one-pot batch system. The successful

application of statistical design models enabled improved production from phylogenetically distinct microbes. PDO and WEs were extracted from the fermentation broth, broadening crude glycerol valorization profile. To our knowledge, this is the first report to demonstrate WE synthesis from crude glycerol. Future studies will focus on the repeatability of the process, and its effect on the cellular maintenance and WE accumulation in *A. baylyi* cells using a fed-batch process.

Appendix A. Supplementary data

Supplementary data related to this article is included with the submission.

Acknowledgements

References

[1]   EU Sugar Market Observatory. AGRI G 4, The C for, Markets CO of A. Sugar price reporting n.d. https://ec.europa.eu/agriculture/market-observatory/sugar/statistics_en (accessed November 26, 2018).

[2]   Oleoline. Crude Glycerin Market Report. July 30 2018. https://www.oleoline.com/products/Crude-Glycerine-Market-Report-7.html (accessed November 26, 2018).

[3]   Quispe CAG, Coronado CJR, Carvalho Jr. JA. Glycerol: Production, consumption, prices, characterization and new trends in combustion. Renew Sustain Energy Rev 2013;27:475–93. doi:10.1016/j.rser.2013.06.017.

[4]   Burniol-Figols A, Varrone C, Le SB, Daugaard AE, Skiadas I V., Gavala HN. Combined polyhydroxyalkanoates (PHA) and 1,3-propanediol production from crude glycerol: Selective conversion of volatile fatty acids into PHA by mixed microbial consortia. Water Res 2018;136:180–91. doi:10.1016/j.watres.2018.02.029.

[5]   Choi WJ, Hartono MR, Chan WH, Yeo SS. Ethanol production from biodiesel-derived crude

glycerol by newly isolated Kluyvera cryocrescens. Appl Microbiol Biotechnol 2011;89:1255–64. doi:10.1007/s00253-010-3076-3.

[6]   Chatzifragkou A, Aggelis G, Komaitis M, Zeng AP, Papanikolaou S. Impact of anaerobiosis strategy and bioreactor geometry on the biochemical response of Clostridium butyricum VPI 1718 during 1,3-propanediol fermentation. Bioresour Technol 2011;102:10625–32. doi:10.1016/j.biortech.2011.09.023.

[7]   Huang J, Wu Y, Wu W, Zhang Y, Liu D, Chen Z. Cofactor recycling for co-production of 1,3-propanediol and glutamate by metabolically engineered Corynebacterium glutamicum. Sci Rep 2017;7. doi:10.1038/srep42246.

[8]   Lee CS, Aroua MK, Daud WMAW, Cognet P, Pérès-Lucchese Y, Fabre P-L, et al. A review: Conversion of bioglycerol into 1,3-propanediol via biological and chemical method. Renew Sustain Energy Rev 2015;42:963–72. doi:10.1016/j.rser.2014.10.033.

[9]   Cecilia, Juan A., Garcia-Sancho, Cristina., Maireles-Torres, Pedro J., Luque R. Foodwaste as Feedstock. First Edit. Cham: Springer International Publishing; 2019. doi:10.1007/978-3-030-10961-5.

[10]   MarketsANDMarkets. 1, 3-Propanediol (PDO) Market by Applications (PTT, Polyurethane, Cosmetic, Personal Care & Home Cleaning & Others) & Geography - Global Market Trends & Forecasts to 2021 n.d. https://www.marketsandmarkets.com/Market-Reports/1-3-propanediol-pdo-market-760.html (accessed November 26, 2018).

[11]   Knifton JF, James TG, Slaugh LH, Allen KD, Weider PR, Allen KD, Powell, JB. One-step production of 1,3-Propanediol from ethylene oxide and syngas with a cobalt-iron catalyst. 2009. US Patent No. US7538061B2. https://patents.google.com/patent/US7538061/it

[12]   Besson M, Gallezot P, Pigamo A, Reifsnyder S. Development of an improved continuous

hydrogenation process for the production of 1,3-propanediol using titania supported ruthenium catalysts. Appl Catal A Gen 2003;250:117–24. doi:10.1016/S0926-860X(03)00233-3.

[13]   Wilkens E, Ringel AK, Hortig D, Willke T, Vorlop KD. High-level production of 1,3-propanediol from crude glycerol by Clostridium butyricum AKR102a. Appl Microbiol Biotechnol 2012;93:1057–63. doi:10.1007/s00253-011-3595-6.

[14]   Papanikolaou S, Ruiz-Sanchez P, Pariset B, Blanchard F, Fick M. High production of 1,3-propanediol from industrial glycerol by a newly isolated Clostridium butyricum strain. J Biotechnol 2000;77:191–208. doi:10.1016/S0168-1656(99)00217-5.

[15]   Jensen TØ, Kvist T, Mikkelsen MJ, Westermann P. Production of 1,3-PDO and butanol by a mutant strain of Clostridium pasteurianum with increased tolerance towards crude glycerol. AMB Express 2012;2:1–7. doi:10.1186/2191-0855-2-44.

[16]   Wischral D, Zhang J, Cheng C, Lin M, De Souza LMG, Pessoa FLP, et al. Production of 1,3-propanediol by Clostridium beijerinckii DSM 791 from crude glycerol and corn steep liquor: Process optimization and metabolic engineering. Bioresour Technol 2016;212:100–10. doi:10.1016/j.biortech.2016.04.020.

[17]   Leng L, Yang P, Mao Y, Wu Z, Zhang T, Lee PH. Thermodynamic and physiological study of caproate and 1,3-propanediol co-production through glycerol fermentation and fatty acids chain elongation. Water Res 2017;114:200–9. doi:10.1016/j.watres.2017.02.023.

[18]   Alibaba. Wholesale Bulk Pure Jojoba Seed Extract Jojoba Oil Price n.d. https://www.alibaba.com/product-detail/Wholesale-Bulk-Pure-Jojoba-Seed-Extract_62030803572.html?spm=a2700.7724857.normalList.7.338d78a1H2lmq1&s=p (accessed June 19, 2019).

[19]   Research GV. Jojoba Oil Market Projected To Reach $254.2 Million By 2024 n.d.

https://www.grandviewresearch.com/press-release/global-jojoba-oil-market (accessed December 10, 2018).

[20] Kannisto M, Efimova E, Karp M, Santala V. Growth and wax ester production of an Acinetobacter baylyi ADP1 mutant deficient in exopolysaccharide capsule synthesis. J Ind Microbiol Biotechnol 2017;44:99–105. doi:10.1007/s10295-016-1872-1.

[21] Kannisto M, Aho T, Karp M, Santala V. Metabolic engineering of Acinetobacter baylyi ADP1 for improved growth on gluconate and glucose. Appl Environ Microbiol 2014;80:7021–7. doi:10.1128/AEM.01837-14.

[22] Santala S, Efimova E, Koskinen P, Karp MT, Santala V. Rewiring the Wax Ester Production Pathway of Acinetobacter baylyi ADP1. ACS Synth Biol 2014;3:145–51. doi:10.1021/sb4000788.

[23] Fixter LM, Nagi MN, Mccormack JG, Fewson C a. Structure, Distribution and Function of Wax Esters in Acinetobacter calcoaceticus. Microbiology 1986;132:3147–57. doi:10.1099/00221287-132-11-3147.

[24] Santala S, Karp M, Santala V. Rationally Engineered Synthetic Coculture for Improved Biomass and Product Formation. PLoS One 2014;9:e113786. doi:10.1371/journal.pone.0113786.

[25] Salmela M, Lehtinen T, Efimova E, Santala S, Mangayil R. Metabolic pairing of aerobic and anaerobic production in a one-pot batch cultivation. Biotechnol Biofuels 2018;11:187. doi:10.1186/s13068-018-1186-9.

[26] Seppälä JJ, Puhakka JA, Yli-Harja O, Karp MT, Santala V. Fermentative hydrogen production by Clostridium butyricum and Escherichia coli in pure and cocultures. Int J Hydrogen Energy 2011;36:10701–8. doi:10.1016/j.ijhydene.2011.05.189.

[27] Plackett RL, Burman JP. The Design of Optimum Multifactorial Experiments. Biometrika 1946;33:305–25. doi:10.2307/2332195.

[28]   Box GEP, Behnken DW. Some New Three Level Designs for the Study of Quantitative Variables. Technometrics 1960;2:455–75. doi:10.1080/00401706.1960.10489912.

[29]   Lehtinen T, Efimova E, Santala S, Santala V. Improved fatty aldehyde and wax ester production by overexpression of fatty acyl-CoA reductases. Microb Cell Fact 2018. doi:10.1186/s12934-018-0869-z.

[30]   Mangayil R, Santala V, Karp M. Fermentative hydrogen production from different sugars by Citrobacter sp. CMC-1 in batch culture. Int J Hydrogen Energy 2011;36:15187–94. doi:10.1016/j.ijhydene.2011.08.076.

[31]   Wischral D, Fu H, Pellegrini Pessoa FL, Pereira N, Yang ST. Effective and simple recovery of 1,3-propanediol from a fermented medium by liquid–liquid extraction system with ethanol and K3PO4. Chinese J Chem Eng 2018;26:137–43. doi:10.1016/j.cjche.2017.06.005.

[32]   Kannisto MS, Mangayil RK, Shrivastava-Bhattacharya A, Pletschke BI, Karp MT, Santala VP. Metabolic engineering of Acinetobacter baylyi ADP1 for removal of Clostridium butyricum growth inhibitors produced from lignocellulosic hydrolysates. Biotechnol Biofuels 2015;8:198. doi:10.1186/s13068-015-0389-6.

[33]   Durot M, Le Fèvre F, de Berardinis V, Kreimeyer A, Vallenet D, Combe C, et al. Iterative reconstruction of a global metabolic model of Acinetobacter baylyi ADP1 using high-throughput growth phenotype and gene essentiality data. BMC Syst Biol 2008;2:85. doi:10.1186/1752-0509-2-85.

[34]   Liu Y, Ding M, Ling W, Yang Y, Zhou X, Li B-Z, et al. A three-species microbial consortium for power generation. Energy Environ Sci 2017;10:1600–9. doi:10.1039/C6EE03705D.

[35]   Sgobba E, Stumpf AK, Vortmann M, Jagmann N, Krehenbrink M, Dirks-Hofmeister ME, et al. Synthetic Escherichia coli - Corynebacterium glutamicum consortia for l- lysine production from

starch and sucrose. Bioresour Technol 2018;260:302–10. doi:10.1016/j.biortech.2018.03.113.

[36] Zhu C, Fang B, Wang S. Effects of culture conditions on the kinetic behavior of 1,3-propanediol fermentation by Clostridium butyricum with a kinetic model. Bioresour Technol 2016. doi:10.1016/j.biortech.2016.04.028.

[37] Moscoviz R, Trably E, Bernet N. Consistent 1,3-propanediol production from glycerol in mixed culture fermentation over a wide range of pH. Biotechnol Biofuels 2016. doi:10.1186/s13068-016-0447-8.

[38] Himmi EH, Bories A, Barbirato F. Nutrient requirements for glycerol conversion to 1,3-propanediol by Clostridium butyricum. Bioresour Technol 1999. doi:10.1016/S0960-8524(98)00109-6.

[39] Günzel B, Yonsel S, Deckwer W-D. Fermentative production of 1,3-propanediol from glycerol by Clostridium butyricum up to a scale of 2m3. Appl Microbiol Biotechnol 1991;36:289–94. doi:10.1007/BF00208143.

[40] Mangayil R, Aho T, Karp M, Santala V. Improved bioconversion of crude glycerol to hydrogen by statistical optimization of media components. Renew Energy 2015;75:583–9. doi:10.1016/j.renene.2014.10.051.

[41] Lenth R V. Response-Surface Methods in R , Using rsm. J Stat Softw 2009;32:1–17. doi:10.18637/jss.v032.i07.

[42] Bizukojc M, Dietz D, Sun J, Zeng AP. Metabolic modelling of syntrophic-like growth of a 1,3-propanediol producer, Clostridium butyricum, and a methanogenic archeon, Methanosarcina mazei, under anaerobic conditions. Bioprocess Biosyst Eng 2010. doi:10.1007/s00449-009-0359-0.

[43] Papanikolaou S, Fick M, Aggelis G. The effect of raw glycerol concentration on the production of 1,3-propanediol by Clostridium butyricum. J Chem Technol Biotechnol 2004;79:1189–96. doi:10.1002/jctb.1103.

[44] Wenning L, Yu T, David F, Nielsen J, Siewers V. Establishing very long-chain fatty alcohol and wax ester biosynthesis in Saccharomyces cerevisiae. Biotechnol Bioeng 2017. doi:10.1002/bit.26220.

[45] Volker AR, Gogerty DS, Bartholomay C, Hennen-Bierwagen T, Zhu H, Bobik TA. Fermentative production of short-chain fatty acids in Escherichia coli. Microbiol (United Kingdom) 2014. doi:10.1099/mic.0.078329-0.
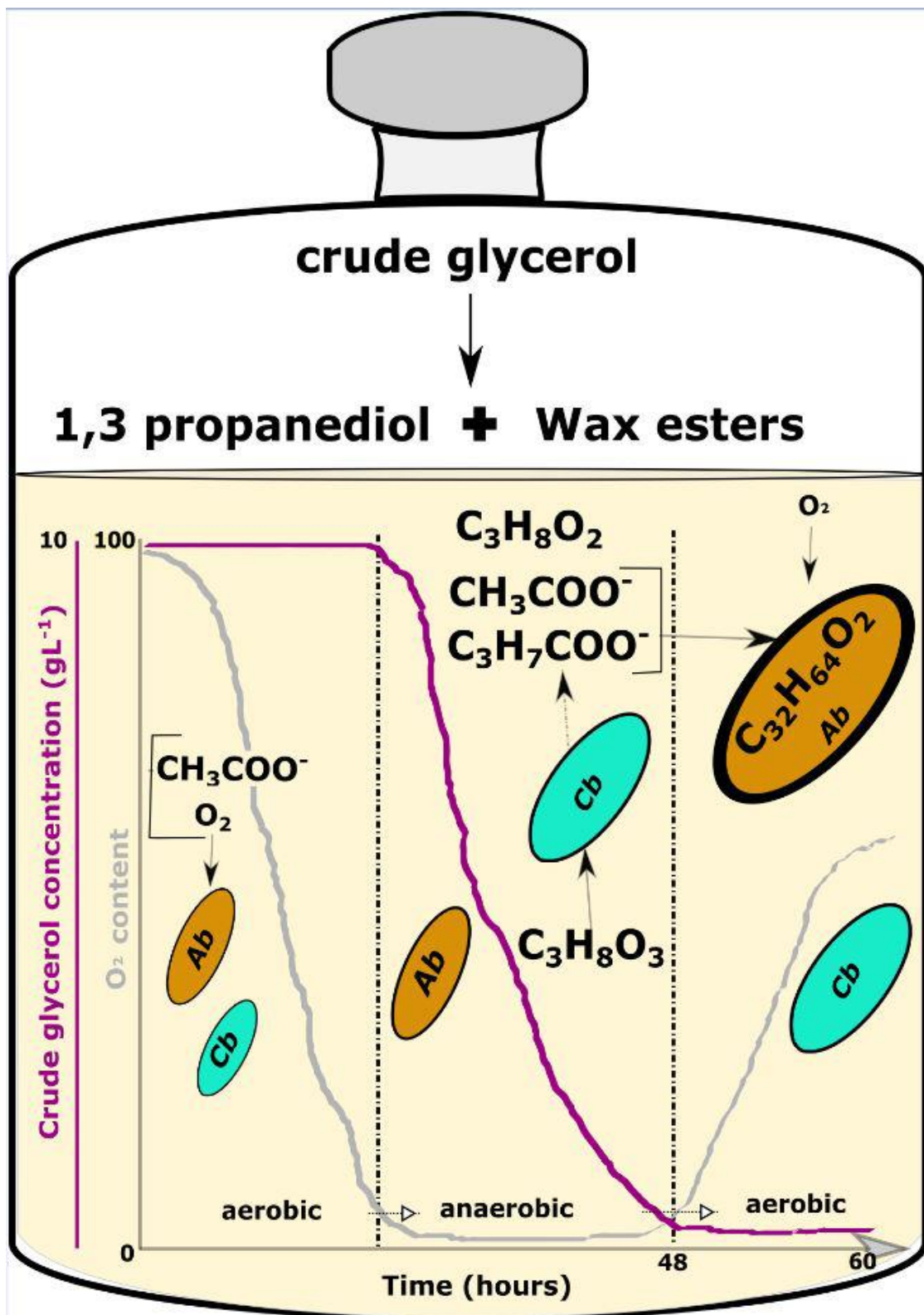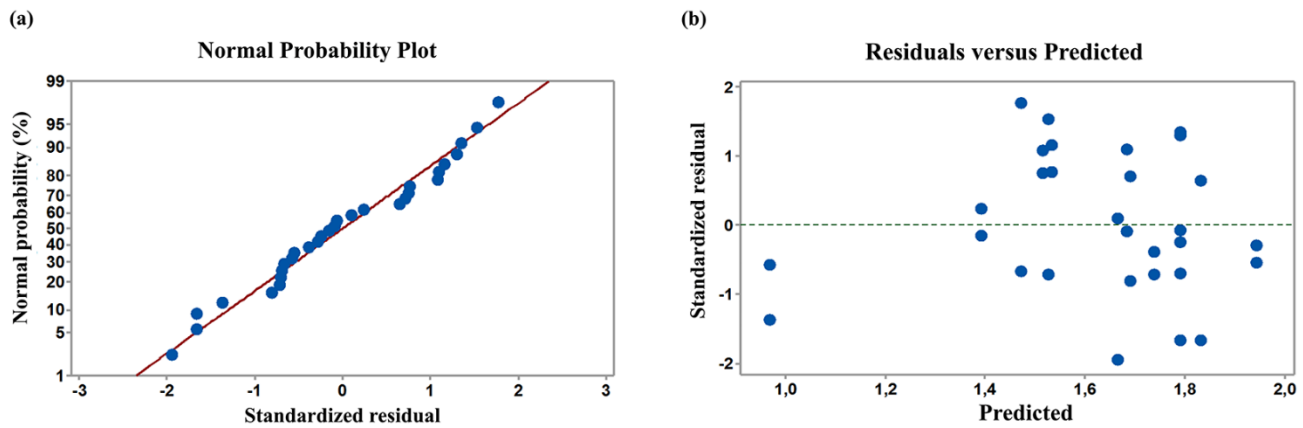
Figure 1. Residual plots to examine the goodness-of-fit of *A. baylyi* ADP1 growth response surface regression model. The normal probability plot (a) verifies the normal distribution of model residuals. The residual versus predicted plot (b) shows the random scatter of residuals along the ascending predicted values around the centerline.
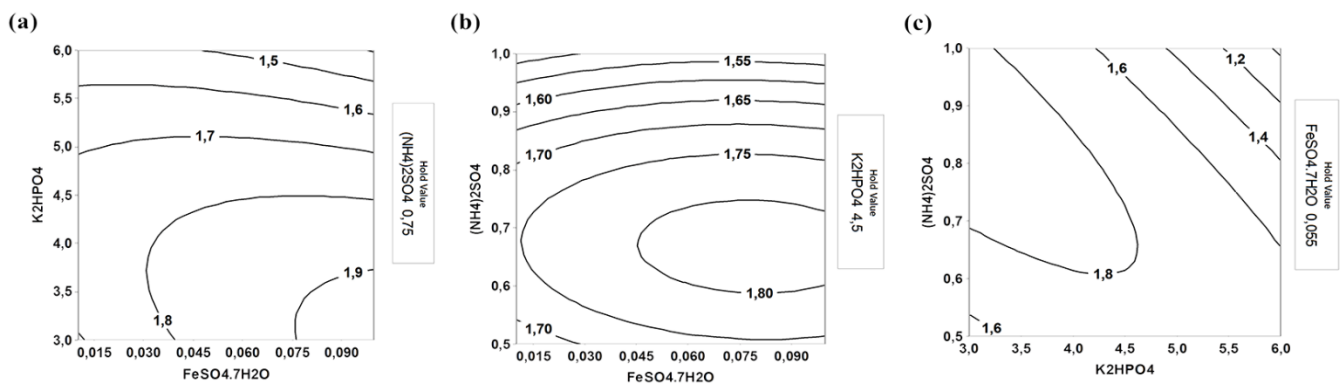
Figure 2. The interaction effects of $FeSO_4.7H_2O$; K_2HPO_4, and $(NH_4)_2SO_4$ on *A. baylyi* ADP1 growth. The concentrations (g L^{-1}) of the model variables ($FeSO_4.7H_2O$; K_2HPO_4, and $(NH_4)_2SO_4$) are presented on the x and y-axes. $FeSO_4.7H_2O:K_2HPO_4$, $FeSO_4.7H_2O:(NH_4)_2SO_4$ and $K_2HPO_4:(NH_4)_2SO_4$ interactions on the response are presented in sub-figures a, b, and c, respectively. The predicted values for *A. baylyi* ADP1 growth (OD_{600nm}) are shown on the contour lines. The legend on each contour plot specifies the hold value of the third variable.

27

Table 1. Plackett-Burman design and experimental results. The anaerobic and aerobic phases represent the data after *C. butyricum* fermentation and *A. baylyi* growth from *C. butyricum* metabolites. The averaged values ± standard deviations from duplicate cultivations are presented.

Run	Variables [a]						Initial pH	Anaerobic phase							Aerobic phase		
	A	B	C	D	E	F		OD	pH	Ace mM	But mM	CG %	PDO mM	PDO$_{predicted}$	pH	OD [b]	OD$_{predicted}$
1	+	+	-	+	+	-	7.7	1.4±0.0	6.9	3.4±0.0	4.5±0.1	100±0.0	21.1±0.2	21.8	8.1	0.2±0.0	0.2
2	-	+	+	+	-	+	7.2	2.4±0.1	5.2	7.2±0.0	7.4±0.2	53±0.4	44.9±0.1	44.7	5.2	NG	-0.1
3	+	+	-	+	-	-	7.7	1.5±0.0	7.7	3.5±0.1	4.7±0.1	100±0.0	21.1±0.1	22.8	7.9	0.2±0.0	0.3
4	+	+	+	-	+	+	7.7	2.4±0.3	7.7	5.2±0.5	8.6±0.0	46±0.1	47.4±1.0	48.5	7.2	0.5±0.1	0.7
5	-	-	-	+	+	+	7.4	2.3±0.1	7.4	6.8±0.1	8.7±0.2	60±0.5	48.6±1.0	48.8	5.2	0.1±0.0	0.2
6	-	-	+	+	+	-	7.4	1.5±0.0	7.4	3.4±0.1	4.5±0.1	100±0.0	21.5±0.3	23.9	7.6	0.3±0.0	0.4
7	-	+	+	-	+	-	7.3	1.6±0.0	5.3	3.9±0.1	4.5±0.1	100±0.0	21.7±0.3	23.1	7.7	NG	-0.1
8	-	-	-	-	-	-	7.4	1.6±0.0	7.4	3.4±0.1	4.6±0.2	100±0.0	21.3±0.4	29.2	7.6	0.2±0.0	0.7
9	+	-	+	+	-	+	7.8	2.3±0.1	7.8	6.5±1.0	11.0±2.0	62±1.0	47.9±0.0	50.3	6.8	1.2±0.1	1.3
10	-	+	-	-	-	+	7.2	2.3±0.1	5.1	6.8±0.0	9.1±0.1	51±0.9	46.5±0.3	48.9	5.2	NG	-0.1
11	0	0	0	0	0	0	7.6	1.7±0.0	6.1	5.5±0.2	8.6±0.0	100±0.0	41.3±0.0	34.5	7.0	1.0±0.0	0.6
12	0	0	0	0	0	0	7.6	1.7±0.0	6.1	5.1±0.1	8.9±0.1	100±0.0	41.6±0.0	34.5	6.8	1.1±0.0	0.6
13	0	0	0	0	0	0	7.6	1.8±0.0	6.1	5.1±0.0	8.8±0.1	100±0.0	41.8±0.0	34.5	6.9	1.0±0.0	0.6
14	+	-	-	-	+	+	7.9	2.2±0.0	6.3	7.3±0.1	11±0.5	68±0.3	52.3±1.8	53.6	7.1	1.2±0.1	1.2

[a] Factors: A, K_2HPO_4; B, $(NH_4)_2SO_4$; C, $MgSO_4.7H_2O$; D, $CaCl_2.2H_2O$; E, $FeSO_4.7H_2O$ and F, Crude glycerol.

[b] OD from the 48-hour anaerobic phase deducted from the final OD data.

Ace mM and But mM, millimolar concentrations of acetate and butyrate; CG %, crude glycerol utilization percentage, PDO, 1,3 propanediol;

OD, optical density measured at wavelength of 600nm, NG, no growth, PDO$_{predicted}$ and OD$_{predicted}$, model predicted values.

Table 2. Experimental design and results for three-variable Box-Behnken optimization conducted using *A. baylyi* ADP1 – *C. butyricum* co-cultures are presented. The anaerobic and aerobic phases presents the observed data after *C. butyricum* fermentation and the by-product utilization by *A. baylyi* ADP1, respectively. The averaged values ± standard deviations from duplicate cultivations are presented. The concentrations of other JM medium components are 0.4 g L^{-1} $MgSO_4.7H_2O$, 0.0075 g L^{-1} $CaCl_2.2H_2O$, 10 g L^{-1} crude glycerol, 0.3 g L^{-1} yeast extract, 2 ml L^{-1} TE solution and 10mM acetate.

Run	Variables [a]			Anaerobic phase								Aerobic phase		
	A	B	C	Initial pH	OD	pH	Ace mM	But mM	CG (%)	PDO mM	PDO$_{predicted}$	pH	OD[b]	OD$_{predicted}$
1	-1	0	1	8.0±0.1	2.1±0.0	6.7±0.1	6.1±0.4	10.6±1.8	80.0±0.3	55.6±1.9	55.0	7.1±0.1	1.6±0.3	1.5
2	0	1	1	8.0±0.1	1.9±0.4	6.7±0.0	5.5±0.2	11.1±0.1	78.3±0.9	53.0±0.6	54.5	7.1±0.6	0.8±0.1	1.0
3	-1	-1	0	7.9±0.0	2.3±0.1	6.3±0.0	5.9±0.5	11.9±0.8	85.3±0.7	57.7±3.9	58.4	6.6±0.4	1.7±0.2	1.7
4	1	1	0	8.0±0.1	1.7±0.1	6.7±0.0	5.5±0.5	12.1±0.4	84.1±3.8	57.2±2.3	56.5	7.2±0.0	1.4±0.1	1.4
5	1	0	1	7.9±0.0	1.7±0.1	6.6±0.1	6.0±0.4	12.0±1.0	84.7±5.3	57.5±4.3	56.7	7.2±0.1	1.7±0.1	1.5
6	-1	0	-1	8.0±0.0	2.2±0.2	6.6±0.1	5.5±0.0	12.5±1.0	87.8±5.5	58.5±3.1	59.4	7.2±0.1	1.5±0.2	1.7
7	0	-1	-1	7.9±0.0	2.2±0.1	6.3±0.1	5.9±0.3	12.2±0.5	87.9±2.5	58.3±2.8	56.9	7.2±0.1	1.7±0.1	1.5
8	1	0	-1	8.0±0.1	1.8±0.0	6.4±0.1	5.4±0.8	12.6±2.2	86.2±2.3	55.8±0.4	55.5	7.2±0.1	1.8±0.2	1.7
9	-1	1	0	8.0±0.0	2.1±0.1	6.7±0.0	5.6±0.3	12.1±0.5	83.9±3.8	57.1±2.8	56.2	7.3±0.1	1.6±0.2	1.5
10	0	1	-1	8.0±0.0	1.7±0.0	6.7±0.0	5.3±0.6	11.9±0.6	81.7±1.0	55.1±2.1	55.2	7.4±0.1	1.8±0.1	1.7
11	0	-1	1	7.8±0.0	1.9±0.0	6.4±0.2	5.7±0.1	11.0±1.0	82.3±7.3	54.6±3.5	54.5	7.0±0.0	1.8±0.3	1.8
12	1	-1	0	7.8±0.0	1.7±0.1	6.3±0.0	5.2±0.4	11.4±0.2	81.2±4.7	55.1±1.4	56.0	7.1±0.0	1.9±0.0	1.9
13	0	0	0	7.9±0.0	1.8±0.2	6.5±0.1	5.5±0.2	12.2±0.7	84.8±5.3	57.9±3.4	57.3	7.2±0.0	1.9±0.2	1.8
14	0	0	0	7.9±0.0	1.9±0.1	6.6±0.0	5.3±0.2	12.1±0.2	86.2±0.9	57.6±0.3	57.3	7.2±0.1	1.8±0.4	1.8
15	0	0	0	8.0±0.0	2.0±0.1	6.6±0.1	6.3±0.3	11.9±0.1	82.7±0.9	56.5±0.2	57.3	7.1±0.0	1.7±0.1	1.8

[a] A, $FeSO_4.7H_2O$; B, K_2HPO_4, and C, $(NH_4)_2SO_4$.

[b] OD from the 48-hour anaerobic phase deducted from the final OD data.

Table 3. ANOVA for Plackett-Burman model.

Source	df	Adj SS	Adj MS	F-value	p-value	Coefficient (coded)	SE$_{coefficient}$	Effect
				PDO production [a]				
Model	7	2034.66	290.67	360.51	<0.01			
Linear	6	1957.36	326.23	404.61	<0.01			
K_2HPO_4	1	4.41	4.41	5.46	0.04	0.66	0.28	1.32
$(NH_4)_2SO_4$	1	9.29	9.29	11.52	0.02	-0.96	0.28	-1.93
$MgSO_4.7H_2O$	1	1.69	1.69	2.10	0.20	-0.41	0.28	-0.82
$CaCl_2.2H_2O$	1	3.18	3.18	3.94	0.09	-0.56	0.28	-1.13
$FeSO_4.7H_2O$	1	4.71	4.71	5.84	0.05	0.69	0.28	1.37
Crude glycerol	1	1740.98	1740.98	2159.32	<0.01	13.20	0.28	26.39
Curvature	1	234.57	234.57	290.94	<0.01			
Error	6	4.84	0.81					
Lack-of-Fit	4	4.72	1.18	20.44	0.047			
Pure error	2	0.12	0.06					
Total	13	2039.50						
				A. baylyi ADP1 growth [b]				
Model	7	3.33	0.48	38.41	<0.01			
Linear	6	2.16	0.36	29.04	<0.01			
K_2HPO_4	1	1.26	1.26	101.93	<0.01	0.36	1.26	0.71
$(NH_4)_2SO_4$	1	0.85	0.85	68.80	<0.01	-0.29	1.26	-0.58
$MgSO_4.7H_2O$	1	0.17	0.17	13.49	0.01	0.13	1.26	0.26
$CaCl_2.2H_2O$	1	0.09	0.09	7.30	0.04	-0.10	1.26	-0.19
$FeSO_4.7H_2O$	1	0.00	0.00	0.14	0.72	-0.01	1.26	-0.03
Crude glycerol	1	0.04	0.04	3.16	0.13	0.06	1.26	0.13
Curvature	1	0.89	0.89	71.89	<0.01			
Error	6	0.07	0.01					
Lack-of-Fit	4	0.07	0.02	3.50	0.23			
Pure error	2	0.01	0.01					
Total	13	3.4						

[a] S-value, 0.9 mM; R^2, 99.8%; adjusted R^2, 99.5%.

[b] S-value, 0.1 OD$_{600nm}$; R^2, 97.8%; adjusted R^2, 95.3%.

df, degree of freedom; Adj SS, adjusted sum of squares; Adj MS, adjusted mean square; SE$_{coefficient}$, Standard error of coefficient.

Table 4. ANOVA for full quadratic model.

Source	df	Adj SS	F-value	p-value	Coefficient (coded)	SE$_{coefficient}$
PDO production [a]						
Model	9	54.81	0.92	0.53		
$FeSO_4.7H_2O$	1	4.82	0.73	0.40	-0.55	0.64
K_2HPO_4	1	2.60	0.39	0.54	-0.40	0.64
$(NH_4)_2SO_4$	1	9.97	1.52	0.23	-0.79	0.64
$FeSO_4.7H_2O * FeSO_4.7H_2O$	1	1.31	0.20	0.66	0.42	0.94
$K_2HPO_4 * K_2HPO_4$	1	6.86	1.04	0.32	-0.96	0.94
$(NH_4)_2SO_4*(NH_4)_2SO_4$	1	8.70	1.32	0.26	-1.09	0.94
$FeSO_4.7H_2O * K_2HPO_4$	1	3.64	0.55	0.47	0.67	0.91
$FeSO_4.7H_2O *(NH_4)_2SO_4$	1	14.99	2.28	0.15	1.37	0.91
$K_2HPO_4*(NH_4)_2SO_4$	1	1.33	0.20	0.66	0.41	0.91
Error	20	131.43				
Lack-of-Fit	3	17.36	0.86	0.48		
Pure error	17	114.07				
A. baylyi ADP1 growth [b]						
Model	9	1.58	4.78	<0.01		
$FeSO_4.7H_2O$	1	0.01	0.38	0.54	0.03	0.05
K_2HPO_4	1	0.51	13.90	<0.01	-0.18	0.05
$(NH_4)_2SO_4$	1	0.17	4.74	0.03	-0.10	0.05
$FeSO_4.7H_2O * FeSO_4.7H_2O$	1	0.01	0.18	0.68	-0.03	0.07
$K_2HPO_4 * K_2HPO_4$	1	0.11	3.05	0.10	-0.12	0.07
$(NH_4)_2SO_4*(NH_4)_2SO_4$	1	0.20	5.44	0.03	-0.17	0.07
$FeSO_4.7H_2O * K_2HPO_4$	1	0.07	2.02	0.17	-0.10	0.07
$FeSO_4.7H_2O *(NH_4)_2SO_4$	1	0.00	0.01	0.91	-0.01	0.07
$K_2HPO_4*(NH_4)_2SO_4$	1	0.52	14.01	<0.01	-0.25	0.07
Error	20	131.43				
Lack-of-Fit	3	17.36	0.86	0.48		
Pure error	17	114.10				

[a] S-value, 2.6 mM; R^2, 30%; PRESS, 321.0.

[b] S-value. 0.2 OD$_{600nm}$; R^2. 70%; PRESS. 1.6.

df, degree of freedom; Adj SS, adjusted sum of squares; SE$_{coefficient}$, Standard error of coefficient.

Table 5. Products generated from *A. baylyi* ADP1 – *C. butyricum* co-cultures grown in an optimized aerobic JM medium. The cultivations were performed in one-pot batches at 30°C and 300 rpm. The presented results are averaged values ± standard deviations from triplicate cultivations.

	Substrate metabolized and products generated	Yield
	Substrate	
Crude glycerol	110±5.0 mM (10.2 g L^{-1})	
	Products	
Biomass	0.99±0.3 [a]	
Lipids	9.4±1.0 [b]	
PDO	72.0±0.2 [c]	0.65±0.0 [e]
	5.5±0.0 [d]	0.54±0.0 [f]
WEs	68.0±2.8 [c]	0.62±0.0 [e]
	34.4±1.4 [d]	3.4±1.2 [f]
		34.2±3.2 [g]

[a] Dry cell weight, g L^{-1}.

[b] Percentage from biomass.

[c] PDO (mM, calculated value before extraction) and WE (µM) concentrations. WE concentration.

includes total WEs synthesized from initially added acetate and *C. butyricum* by-products.

[d] PDO content (g L^{-1}) obtained by multiplying the concentration with the PDO molecular weight. WE

(mg L^{-1}) obtained by multiplying the WE concentration with the average WE molar mass (506 g mol^{-1}).

[e] PDO and WE yields per mol substrate, mol PDO and µmol WE mol^{-1} crude glycerol.

[f] PDO and WE yields per gram substrate, g PDO and mg WE g^{-1} crude glycerol.

[g] WE yield per gram biomass, mg WE g^{-1} DCW.